Membrane and Cytoplasmic Proteins Are Transported in the Same Organelle Complex during Nematode Spermatogenesis

Thomas M. Roberts,* Fredrick M. Pavalko,* and Samuel Ward‡

*Department of Biological Science, Florida State University, Tallahassee, Florida 32306; and ‡Department of Embryology, Carnegie Institution of Washington, Baltimore, Maryland 21210

Abstract. During the development of pseudopodial spermatozoa of the nematode, *Caenorhabditis elegans*, protein synthesis stops before differentiation is completed. Colloidal gold conjugates of monoclonal antibody SP56, which binds to the surface of spermatozoa, and TR20, which recognizes the major sperm cytoplasmic protein (MSP), were used to label thin sections of testes embedded in Lowicryl K4M in order to follow polypeptides from their synthesis early in spermatogenesis to their segregation to specific compartments of the mature cell. Both antigens are synthesized in primary spermatocytes and are assembled into a unique double organelle, the fibrous body–membranous organelle (FB–MO) complex. However, the antigens are localized in different regions of this FB–MO complex. As described in detail, the assembly of proteins into the FB–MO complex allows both membrane and cytoplasmic components to be concentrated in the spermatids after meiosis. Then, the stepwise disassembly of this transient structure ensures delivery of each component to its final destination in the mature spermatozoan: MSP filaments in the fibrous body depolymerize, releasing MSP into the cytoplasm and the membranous organelles fuse with the plasma membrane, delivering SP56 antigen to the surface.

DIFFERENTIATING cells acquire their specialized structure and function by a combination of differential gene expression and proper localization of gene products within the cell. Progress toward understanding the developmental regulation of gene expression has been substantial (reviewed in reference 7), but the molecular determinants of morphogenesis have been more elusive (see, for examples, references 16 and 32). Spermatogenesis offers an attractive model for the study of cellular morphogenesis. The developing gamete passes through several morphologically distinct intermediates before it completes differentiation into the simple but highly specialized spermatozoon (11). Because transcription of sperm-specific genes often occurs well before the products of those genes are assembled into the maturing cell (reviewed in reference 21), the determinants of assembly and localization can be studied independently of the control of gene expression.

In this paper, we describe the localization of cell-specific gene products in the nonflagellated, pseudopodial spermatozoa of the nematode, *Caenorhabditis elegans*. Sperm development in *C. elegans* proceeds linearly along the tubular gonad so that cells in specific stages of differentiation can be found at predictable positions in every animal examined (34, 40). This feature has allowed us to use two antibodies to sperm-specific proteins (described in the previous paper [38]) as markers to follow selected cellular components from their synthesis early in development to their final localization in the mature spermatozoon. We found that an unusual transient double organelle complex constructed in primary spermatocytes is used to deliver both membrane and cytoplasmic proteins to the fully differentiated cell.

Materials and Methods

Worm Cultivation

Males of *C. elegans* strain CB1490, *him-5* (*el490*), a mutant strain that produces males at high frequency (13) with fully fertile sperm (23), were used as a routine source of sperm. Worms were grown on bacto-agar plates seeded with *Escherichia coli* as described by Brenner (6).

Monoclonal Antibody Production

Methods of production and purification of the two monoclonal antibodies, ABY TR20 and ABY SP56,[1] used in the study are described in the preceeding paper (38).

Indirect Immunofluorescence Assays

Spermatids were dissected from virgin CB1490 males into sperm medium (SM) and activated to undergo spermiogenesis by treatment with 0.5 μM monensin (20). The resulting spermatozoa were fixed in 3% formaldehyde for 24 h, washed in SM that contained 10 mg/ml glycine, and incubated 1–4 h in ABY TR20 or ABY SP56 (50 μg/ml), followed by fluorescein isothiocyanate-conjugated goat anti-mouse Ig (Cappel Laboratories, Cochranville, PA) at 25 μg/ml for 1–2 h. Labeled sperm were examined in a Zeiss standard microscope equipped with epifluorescent illumination.

1. *Abbreviations used in this paper:* ABY, antibody; CGP–ABY, colloidal gold particle–monoclonal antibody; FB, fibrous body; MO, membranous organelle; MSP, major sperm protein; SM, sperm medium.

Preparation of Colloidal Gold Particle-Monoclonal Antibody (CGP-ABY) Conjugates

Colloidal gold particles were prepared according to Baigent and Muller (1). Briefly, 0.2 ml of a 1% solution of $H(AuCl_4)$ were added to 100 ml of 3× distilled water and adjusted to pH 7 with 0.2 M K_2CO_3. After adding 2 ml of absolute ethanol as a catalyst, the solution was sonicated for 5–7 min at maximum intensity in a Biosonic Ultrasonicator (Bronwill Scientific Products, Rochester, NY). This method produced a bright pink solution (A_{max} = 520 nm) comprised of gold particles 5–10 nm in diameter that were stable for several weeks at 4°C.

Monoclonal antibodies were conjugated to colloidal gold particles by the procedure of Romano et al. (29) with slight modification. 1 ml of purified antibody (0.5 mg/ml in SM) was added dropwise to 2.5 ml of CGP solution with stirring at room temperature. After 15 min, 10 mg of bovine serum albumin (BSA) were added and the solution was mixed for 5 min. NaCl was added to a final concentration of 10 mg/ml, and the mixture was centifuged at 1,700 *g* to remove large aggregates and then at 100,000 *g* for 30 min to pellet the CGP-ABY conjugates. The pellet was resuspended in 0.5 ml of SM and used undiluted in cell labeling experiments. CGP-ABY preparations were stored for several days at 4°C without loss of antibody binding activity.

Preparation of Sperm for Labeling in Thin Sections

To obtain cells in early stages of development, intact gonads were dissected from young males into a drop of SM. Spermatids and monensin-activated spermatozoa were obtained as described above. All specimens were prepared on acid-washed coverslips.

Both sperm and gonads were fixed in SM that contained 1% glutaraldehyde plus 1% formaldehyde for 2–6 h, postfixed in 0.1% OsO_4 for 30 min, and embedded in Lowicryl K4M by the method of Carlemalm et al. (9) with ethanol dehydration, resin infiltration, and ultraviolet polymerization done at −20°C.

Sections 70–90-nm thick were cut on a diamond knife and mounted on formvar-and carbon-coated nickel grids. The grids were floated on a drop of SM that contained 1% BSA for 15 min, washed in distilled water, and incubated in CGP-ABY for 2 h. The specimens were washed in distilled water to remove unbound gold particles, stained in uranyl acetate followed by lead citrate, and examined in a Phillips 201 electron microscope operated at 60 kV.

Morphometric Analyses

The plasma membrane surface areas of spermatids and spermatozoa and the area of different parts of the membranous organelle membranes were determined by standard morphometric analysis (39) of electron micrographs prepared as described previously (34). Longitudinal sections through the testis of a male that had recently mated with a hermaphrodite were used so that both spermatids and spermatozoa would be present in the same section. The curvilinear test pattern of Merz (described in reference 39) was used to determine the surface density of each membrane by line and point intersection. This was converted into the surface area per cell by multiplying by the cellular volume, 85 ± 4 μm^3. This volume was determined from light microscopic examination of live spermatids which are nearly spherical cells with a diameter of 5.4 ± 0.08 μm (n = 25). By direct measurement using uptake of ^3H water, the volume of spermatids and spermatozoa is the same (36). This was further confirmed by light microscopic measurement, assuming the spermatozoon is a partial sphere with a cylindrical pseudopod, and confirmed independently by electron microscopic morphometry, which showed that the volume density of spermatids and spermatozoa on the same section was indistinguishable (data not shown). All data presented are ± standard error.

Results

Summary of C. elegans Spermatogenesis

Sperm development in *C. elegans* males has been described in detail by Wolf et al. (40) and Ward et al. (34) and is summarized in Fig. 1. Spermatogenesis occurs linearly along the gonad. Primary spermatocytes develop from spermatogonia at the distal end of the testis and begin their maturation as a syncytium with a central cytoplasmic core, the rachis. At about the mid-point in the gonad, pachytene spermatocytes separate from the rachis and continue meiosis individually.

Karyokinesis in the primary spermatocyte may or may not be accompanied by cytokinesis. If the two secondary spermatocytes remain attached the second meiotic division yields four haploid spermatids per parent cell; if the secondary spermatocytes separate then each gives rise to two spermatids. In either case, the haploid nuclei condense and move to the periphery of the secondary spermatocyte. The spherical spermatids bud off from the parent cell with separation accomplished by coalescence of membrane vesicles at the junction between the spermatid and the residual spermatocyte cytoplasm.

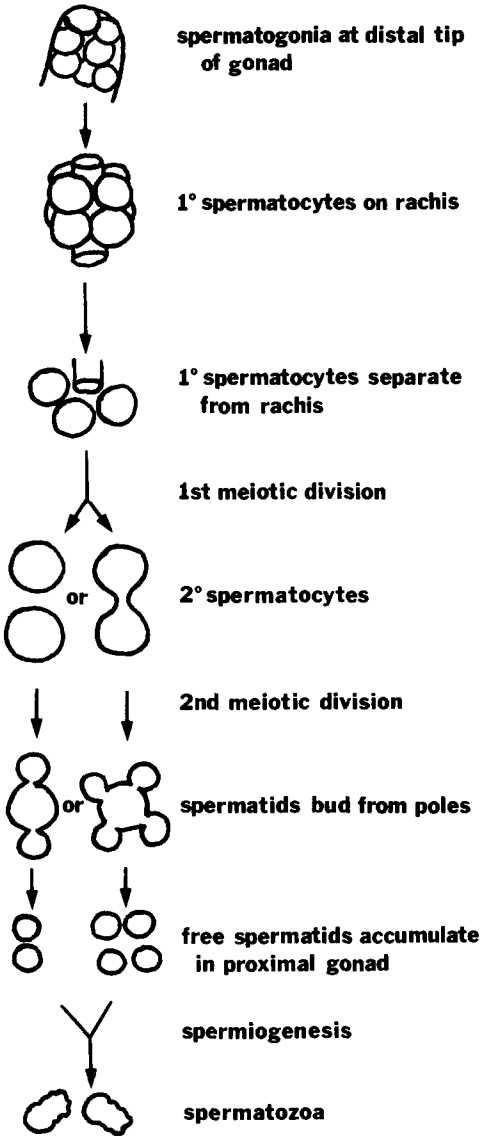

Figure 1. Diagram of spermatogenesis. See text for explanation.

Spermatids accumulate in the proximal portion of the gonad until the male mates. Spermiogenesis is triggered during copulation presumably by a substance secreted from the vas deferens (8). Agents that raise intracellular pH also activate spermiogenesis, as do proteases (23, 36), which results in the formation of a bipolar spermatozoon comprised of a single, persistent pseudopod that extends forward from a hemispherical, organelle-packed cell body.

Spermatozoa contain a highly condensed nucleus, several mitochondria, an extensive system of internal laminar membranes, and numerous membranous organelles (MOs). As

described in detail below, the MOs are constructed early in development as bilobed structures that eventually segregate to the spermatids. During spermiogenesis, they fuse with plasma membrane with one lobe remaining as an inpocket open to the exterior via a permanent fusion pore (see Fig. 8). The abundant microfilaments and microtubules present early in development remain in the residual body when the spermatids are formed (Ward, S., unpublished observations) as do the Golgi complex, endoplasmic reticulum, and ribosomes (34). Spermatids and spermatozoa, therefore, are incapable of protein synthesis so the gene products used to construct the spermatozoon must be synthesized early in spermatogenesis and then segregated to the developing spermatids before they detach from the parent cell.

Localization of the Antigens Recognized by ABYs TR20 and SP56 in Spermatozoa

In the previous paper (38), ABY TR20 was shown to bind exclusively to the major sperm proteins (MSPs). ABY SP56 is one of three monoclonal antibodies that reacts with a set of more than eight different sperm-specific proteins. All three antibodies yield qualitatively similar cell labeling patterns (data not shown), but ABY SP56 consistently labels cells more heavily than the others. Thus, we used ABY SP56 for all immunolabeling experiments in this study.

Labeling of thin sections of Lowicryl-embedded spermatozoa showed that CGP–ABY SP56 binds to the plasma membrane, the MOs, and the pseudopodial cytoplasm (Fig. 2*a*). In contrast, CGP–ABY TR20 labeled the cytoplasm but not the cell surface or any cellular organelles (Fig. 2*b*). The same labeling pattern was obtained by indirect immunofluorescence (Fig. 3). ABY SP56 bound to the plasma membrane of fixed, intact cells yielding a uniform ring of fluorescence around the cell surface and to the inpockets of fused MOs, producing bright spots of fluorescence in the cell body (Fig. 3, *a* and *b*). ABY TR20 failed to label intact spermatozoa (Fig. 3, *c* and *d*) but bound to the cytoplasm, predominantly in the pseudopod, of cells permeabilized by treatment with 0.5% Triton X-100 after fixation (Fig. 3, *e* and *f*). These results establish, first, that the labeling pattern obtained with CGP–ABYs on thin sections faithfully reflects the labeling observed by immunofluorescence and, second, that ABYs SP56 and TR20 bind to separate and distinct parts of the mature cell.

Antigen Localization during Spermatogenesis

The first detectable appearance of antibody labeling during spermatogenesis was binding of CGP–ABY SP56 to two distinct types of membrane-bound structures in primary spermatocytes (Fig. 4, *a* and *b*). One type of vesicle consisted of an electron-lucent core surrounded by a CGP-labeled membrane (Fig. 4*a*). We suspect that these vesicles transport membrane components to the spermatocyte surface because they appeared in the cytoplasm just before we detected CGP–ABY SP56 labeling on the spermatocyte plasma membrane. However, we have not seen these vesicles in the process of fusing with the plasma membrane.

The other labeled organelles in early spermatocytes are the developing MOs. Immature MOs are bilobed structures with the two membrane-bound lobes exhibiting different ABY SP56 labeling patterns (Fig. 4*b*). Gold-conjugated antibody

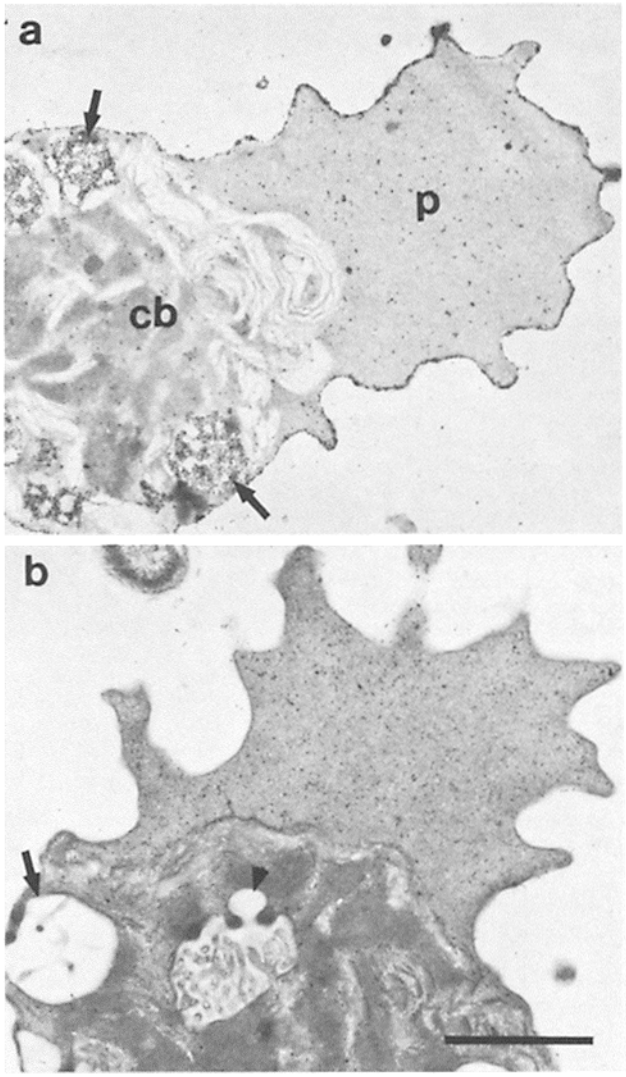

Figure 2. Thin sections of spermatozoa embedded in Lowicryl K4M. (*a*) Labeled with CGP–ABY SP56 showing binding to the plasma membrane, the contents of fused membranous organelles (arrows), within the cell body (*cb*) and the cytoplasm of the pseudopods (*p*); (*b*) Labeled with CGP–ABY TR20. Most of the label is in the granular pseudopod cytoplasm. Neither fused (arrow) nor unfused (arrowhead) membranous organelles are labeled. Bar, 1 μm.

bound to the lumen but not the membrane of the head. The reverse pattern was observed in the body where the surrounding membrane was labeled but the lumen was not. As the MOs matured, the body membranes became more convoluted with the added membrane, like the initial membrane around the body lobe, labeled by ABY SP56 (Figs. 4*c* and 5*d*). The membrane of the head of the MO remained unlabeled.

The first detectable MSP in spermatocytes appeared as patches of granular, ABY TR20-labeled material within the body of the MO (Fig. 5*a*). As development proceeded, these patches enlarged (Fig. 5*b*) and, then, were enveloped by membrane derived from the MO (Fig. 5*c*). The membrane around these patches first appeared as a single layer but later a double membrane, with both layers labeled by ABY SP56, was formed (Fig. 5*d*). The formation of the fibrous body (FB) was marked by the appearance of characteristic parallel arrays

of 4.5-nm filaments wrapped by MO-derived membrane (Fig. 5 *d* and *e*; see also reference 34). As shown in Fig. 5 *e*, CGP-ABY TR20 bound directly to the 4.5-nm filaments so that gold particles overlaid many individual fibers. This confirms the light microscopic evidence of Ward and Klass (35) that MSP is associated closely with these filaments. Determining if the filaments are polymers of MSP will require further experimentation.

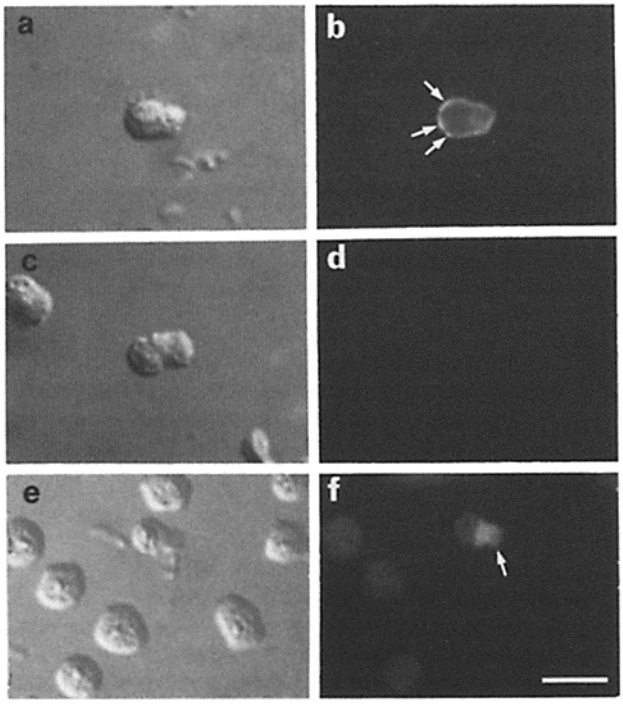

Figure 3. Indirect immunofluorescence labeling of spermatozoa. Left panels, differential interference contrast optics; right panels, same-fields in fluorescence optics. (*a* and *b*) Fixed, intact cell labeled with ABY SP56 showing uniform labeling of the cell surface plus dotted fluorescence where the antibody bound to the MOs (arrows in *b*). (*c* and *d*) Fixed, intact cell labeled with ABY TR20. Note the lack of labeling of the cell surface. (*e* and *f*) Triton X-100 permeabilized cells labeled with ABY TR20. Labeling is particularly heavy in the pseudopod (arrow). Bar, 5 μm.

The ABY SP56 and TR20 labeling patterns established during the assembly of the FB–MO complex persisted as spermatocytes matured. The fibrous bodies enlarged to occupy ~40% of the volume of the secondary spermatocyte (not illustrated; see reference 34). The FB–MO complexes were initially distributed randomly throughout the secondary spermatocyte. However, when spermatids formed as buds at the poles of the secondary spermatocyte, all of the FB–MO complexes moved as units along with the haploid nuclei and the mitochondria to the cytoplasm of the developing spermatids (Fig. 6 *a*). None of the FB–MO complexes were left behind in the residual body in hundreds of residual bodies examined. Numerous membrane-bound vesicles, labeled by ABY SP56, accumulated in the cytoplasm at the junction between the parent cell and the spermatids (Fig. 6 *b*). These vesicles coalesced and fused with the plasma membrane to separate the spermatids from the residual body (Fig. 6 *c*), leaving behind small, ABY SP56-labeled pits at the points of cell separation on the residual body surface (Fig. 6 *d*).

The segregation of components that occurred within the cytoplasm of the secondary spermatocyte during spermatid formation did not take place on the cell surface. Instead, the surface of the residual body was as heavily labeled by ABY SP56 as the surface of the spermatid (Fig. 6 *c*). As a result, much of the antigen assembled onto the spermatocyte surface early in development was lost to the residual body after cytokinesis.

The FB–MO complexes remained intact in the spermatid cytoplasm until after cell separation was completed. Then, the two organelles started to dissociate (Fig. 7). The double membrane around the fibrous body unwrapped and the mem-

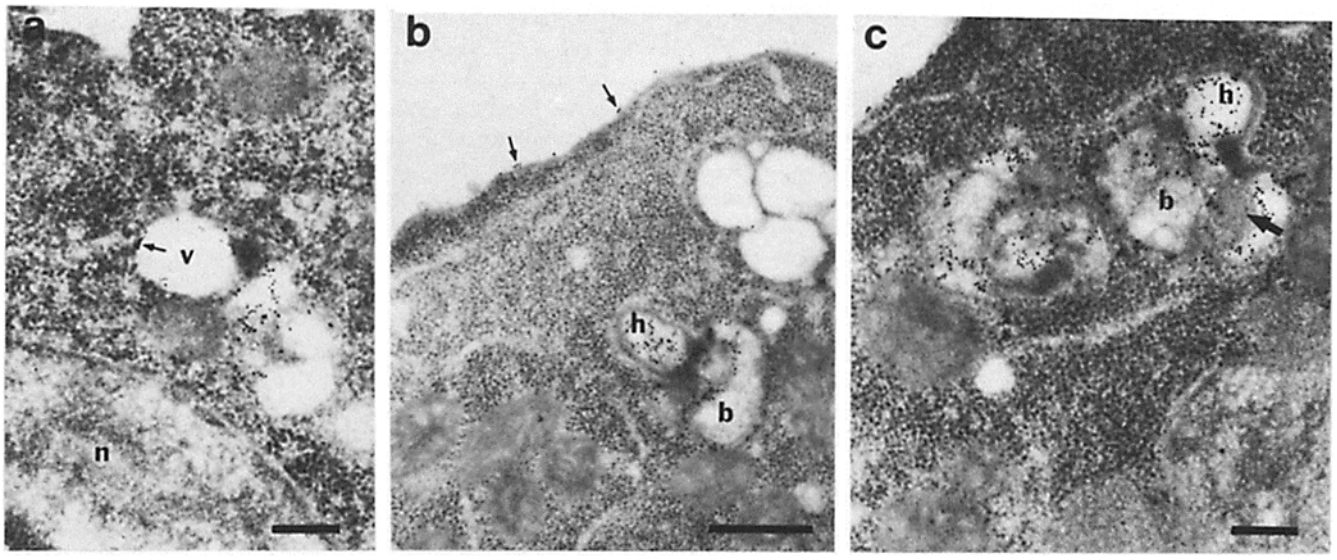

Figure 4. Assembly of the membranous organelles in primary spermatocytes. (*a*) Part of an early primary spermatocyte showing an electron lucent vesicle (*v*) with ABY SP56 labeling (arrow) in the surrounding membrane; *n*, nucleus. (*b*) A primary spermatocyte containing an immature membranous organelle consisting of a spherical head (*h*) and a lobular body (*b*) separated by an electron dense collar. Note the labeling on the cell surface (arrows); (*c*) Two fully-formed MOs exhibiting extensive, ABY SP56-labeled body membranes. Both the head (*h*) and body (*b*) are visible in the MO on the right as is part of the associated fibrous body (arrow). Only the body of the MO on the left is visible in this section. Bars in *a* and *c*, 0.1 μm; bar in *b*, 0.5 μm.

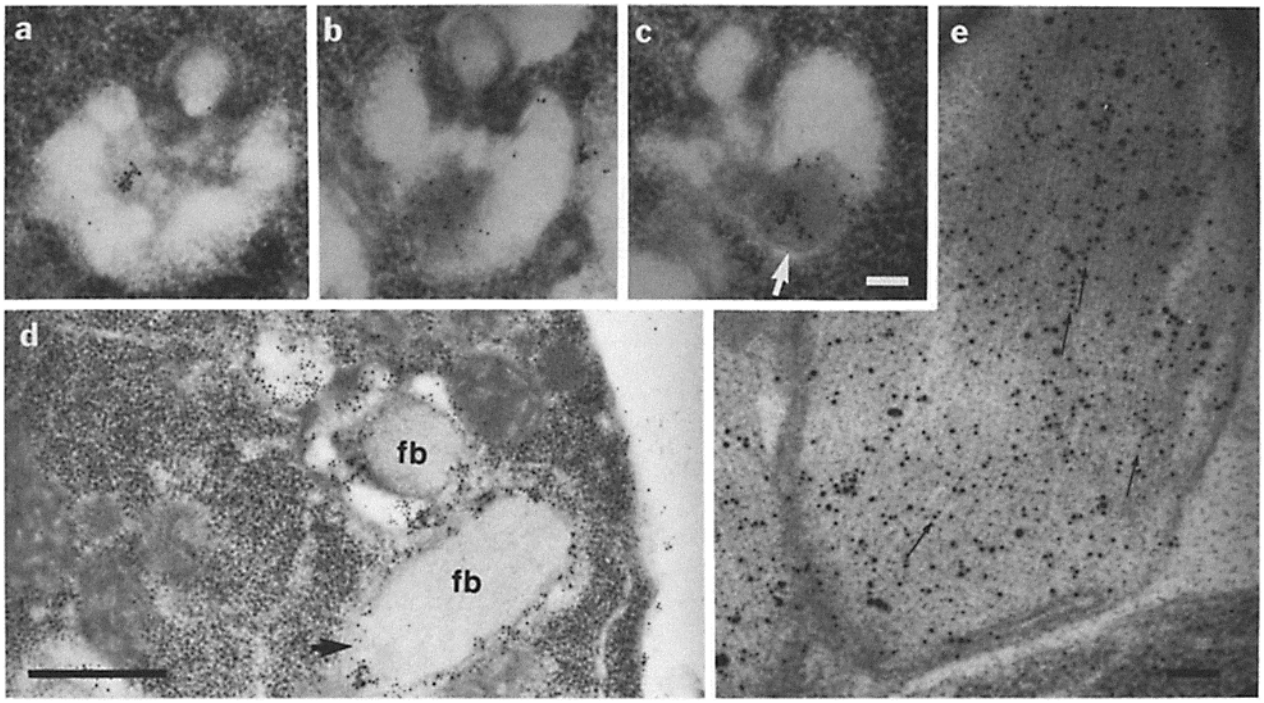

Figure 5. Assembly of the fibrous bodies in primary spermatocytes. (*a–c*) Accumulation of MSP, labeled with ABY TR20, within the body of the MO. Note that in *c* the fibrous body is partly enveloped by membrane (arrow) but that no filaments are evident. (*d*) Mature FB–MO complexes labeled with ABY SP56. The upper complex shows the fibrous body (*fb*) as a parallel array of filaments closely associated with an MO and wrapped by membranes derived from the body of the MO. In the lower complex the only evidence of the MO is the double membrane layer surrounding the oblong fibrous body. Note the gap in the membrane layers (arrow). (*e*) High magnification micrograph of a CGP–ABY TR20-labeled fibrous body showing alignment of gold particles over many of the individual filaments, (arrows). Bars in *c* and *e*, 0.1 μm; bar in *d*, 0.5 μm.

branes pulled back toward the head-body constriction to form the bilobed MO structure characteristic of mature spermatids (Fig. 7, *a*, *b*, and *d*). As the membranes unwrapped and the MOs moved toward the periphery of the cell, the filaments in the now-naked fibrous bodies began to depolymerize as shown by the binding of CGP–ABY TR20 to the cytoplasm adjacent to the remaining filaments (Fig. 7*c*). Disassembly of the fibrous bodies must occur rapidly because we could not find intermediates between cells in which disassembly had just started (Fig. 8*c*) and spermatids that lacked fibrous bodies altogether. The MSP sequestered in the fibrous body dispersed throughout the spermatid cytoplasm after the filaments depolymerized (Fig. 7*e*). Extension of the pseudopod during spermiogenesis resulted in concentration of ABY TR20-labeled MSP in the pseudopod cytoplasm with only a small amount of antigen remaining in the cell body (Fig. 2*b*).

When the MOs moved to the periphery of the spermatid, their heads retained the same ABY SP56 labeling pattern observed earlier in development with binding confined to the granular contents in the lumen (Fig. 8*a*). The finger-like membranes in the body lobe became particularly pronounced. CGP–ABY SP56 aligned along these infolded membranes with the gold particles lying just outside the bilayer, separated from the center of the membrane profile by a gap of 4.0 ± 2.6 nm (n = 54). The same gold particle–membrane orientation was observed on the surface of CGP–ABY SP56-labeled spermatozoa (Fig. 2*a*) where the gold particles bound just external to the plasma membrane separated from the center of the bilayer by 5.7 ± 3.3 nm. These observations suggest that ABY SP56 recognizes an extramembranous epitope of an integral membrane protein in both the plasma membrane and the invaginated membranes in the body of the MO.

The MOs maintained their position along the periphery of the spermatid until the onset of spermiogenesis. During the transition from spermatid to spermatozoon, the MOs fused with the plasma membrane, resulting in the disappearance of the head of the MO and formation of a mass of CGP–ABY SP56 labeled fibers, probably the extruded contents of the head, around the fusion pore (Fig. 8*b*). Much of the invaginated membrane in the body of the MO appeared to be lost after fusion. Morphometric comparison of unfused and fused MOs confirmed this. Fused MOs contained 36% less total membrane than unfused MOs (Table I) due to the disappearance of the head and the loss of about one-half of the invaginated membrane from the lumen of the body. The surface area of the outer membrane of the body did not change after fusion.

The amount of membrane lost from the MO during fusion would be sufficient to increase the surface area of the cell by 64%, but we found that the surface areas of spermatids and spermatozoa were nearly equal (Table II). previous studies have shown that the surface of the spermatozoan pseudopod undergoes continuous centripetal movement accompanied by internalization of membrane components at the cell body–pseudopod junction (28, 37). This removal of membrane from the surface could balance addition of membrane from the

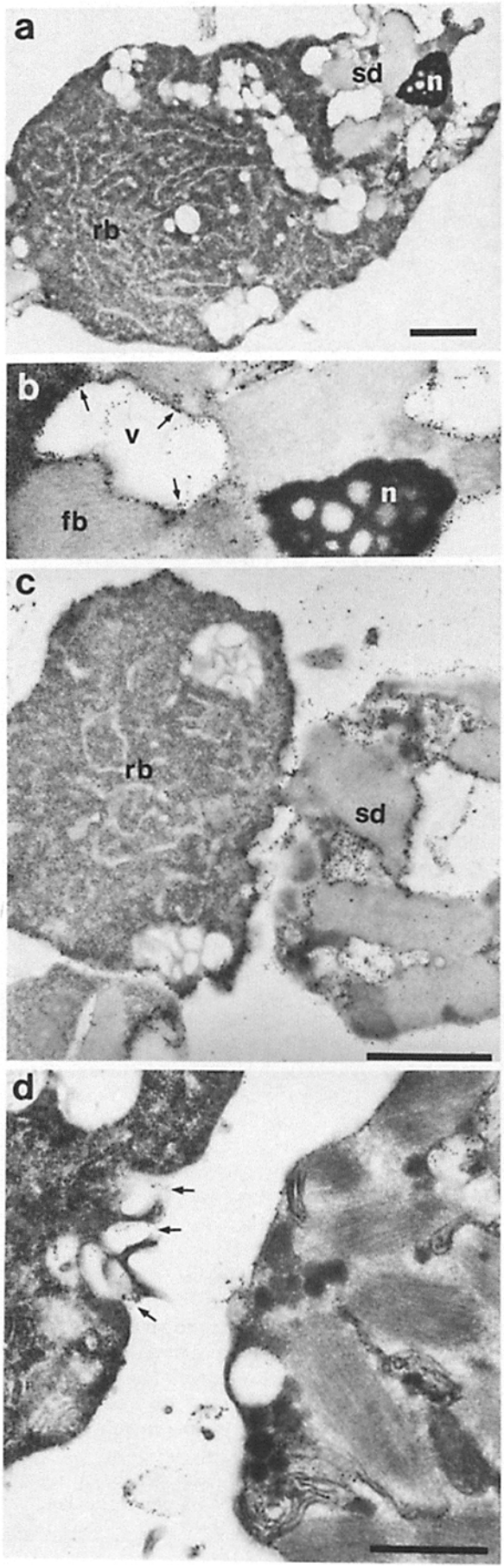

MOs so that there would be no net increase in cellular surface area after MO fusion.

As an alternative method to determine if the antigen recognized by ABY SP56 in the invaginated membranes in the body of the MO was added to the cell surface during spermiogenesis, we removed antigen from the surface of spermatids by treating the cells with sperm medium that contained 200 μg/ml pronase (Boehringer Mannheim Diagnostics, Inc., Houston, TX) for 1 h. Sodium azide (1 mM) was added to the enzyme solution to inhibit protease-induced activation of spermiogenesis (36). Comparison of CGP–ABY SP56-labeled sections of pronase-treated and untreated control spermatids embedded in Lowicryl K4M (Fig. 9, *a* and *b*) shows that proteolytic digestion removed all antibody binding sites from the spermatid surface without altering the binding of antibody to the MOs sequestered in the cytoplasm. Next, pronase-treated cells were washed and stimulated to differentiate into spermatozoa and then fixed and embedded. Treatment of sections of these cells with CGP–ABY SP56 showed that antigen reappeared on the plasma membrane (Fig. 9*c*) as evidenced by gold labeling of the surface of both the pseudopod and the cell body. Because the only nonsurface ABY SP56-labeling in spermatids is in the MOs, this result indicates that the membranous components of the MO body must be added to the plasma membrane during spermiogenesis.

This interpretation was confirmed by examination of the labeling pattern on pronase-treated *fer-1* mutant sperm, cells that fail to fuse their MOs with the cell surface during spermiogenesis (34). Pronase treatment abolished the binding of ABY SP56 to the plasma membrane of *fer-1* spermatids (Fig. 9, *d* and *e*) as it did on wild-type cells. In contrast to wild type, activation of *fer-1* mutant sperm with monensin failed to trigger MO fusion and, as a result, no new antigen could be detected on the surface of the spermatozoon (Fig. 9*f*).

Discussion

Spermatogenesis is an unusual developmental process because, except for a few postmeiotically expressed genes (4, 10, 17), nuclear transcriptional activity ceases before the construction of the spermatozoon is completed (reviewed in reference 3). One way flagellated spermatozoa overcome the time lag between expression of sperm-specific genes and localization of the products of those genes is to synthesize stable mRNA transcripts early in development and delay translation until after the start of spermiogenesis (12, 14, 15, 21). This strategy is not available to nematode sperm because the protein synthesizing machinery fails to segregate to developing sperma-

Figure 6. Formation of spermatids. (*a*) Low magnification view showing a spermatid (*sd*) budding from a secondary spermatocyte. Part of a second spermatid is visible at the opposite pole of the residual body. The condensed nucleus (*n*) and FB–MO complexes have segregated to the developing spermatid, and electron lucent vesicles have begun to accumulate in the spermatocyte cytoplasm. (*b*) Higher magnification view of part of the cell shown in *a*. Note the electron lucent vesicles (*v*) labeled with CGP–ABY SP56, (arrows); *fb*, fibrous body. (*c*) Spermatid (*sd*) separated from the residual body (*rb*). The surfaces of both the spermatid and the residual body are labeled heavily by ABY SP56 as are the membranous portions of the MOs in the spermatid. (*d*) The point where the spermatid separates from the residual body is marked by ABY SP56-labeled pits (arrows). Bars in *a* and *c*, 1 μm; bar in *d*, 0.5 μm.

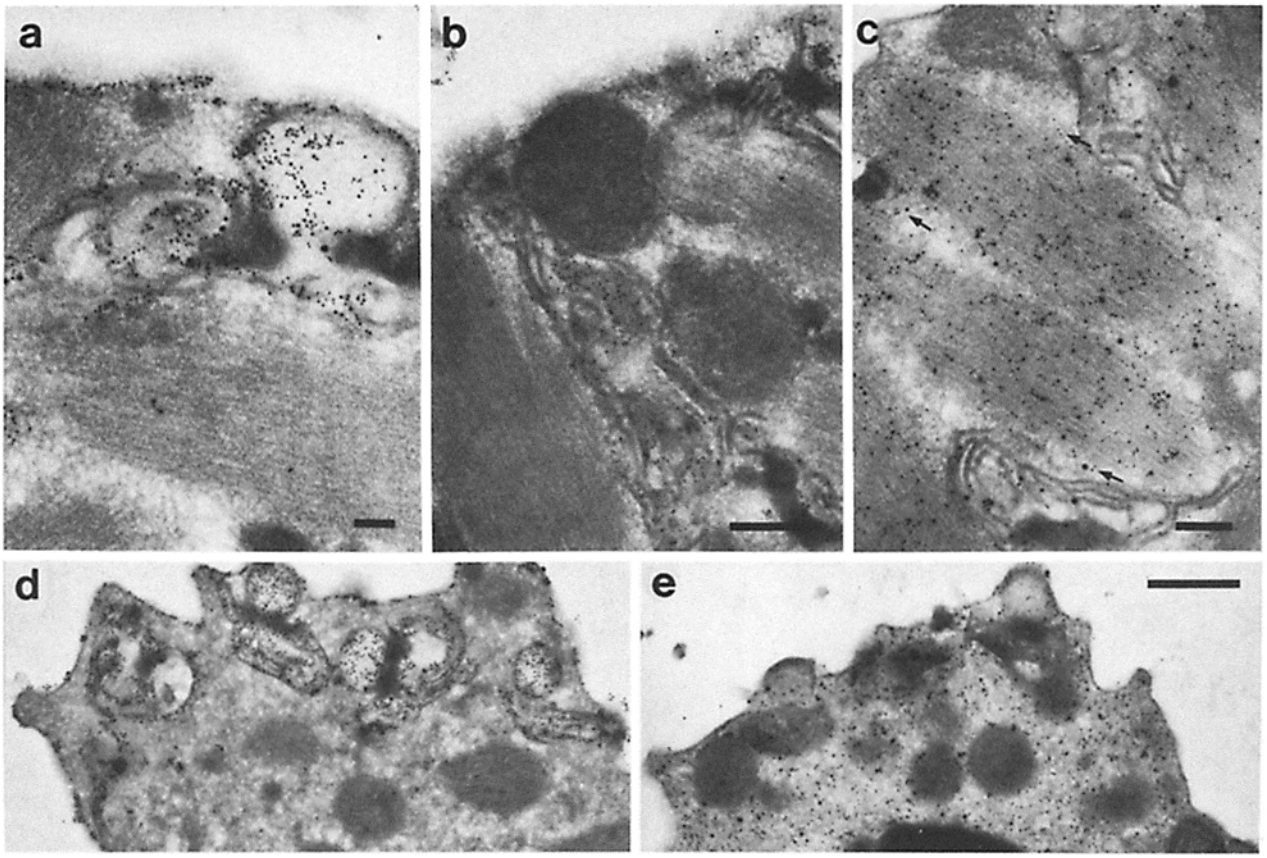

Figure 7. Disassembly of the FB–MO complex in spermatids. (*a*) A spermatid, shortly after separation from the residual body, labeled with ABY SP56. The MO-derived membranes upwrap from the fibrous body and start to pull back toward the head of the MO. (*b*) The same cell showing extensive MO membranes labeled with ABY SP56 and an adjacent, naked fibrous body. (*c*) Near-naked fibrous bodies labeled with ABY TR20. The appearance of gold particles in the cytoplasm (arrows) adjacent to the fibrous body marks the start of filament depolymerization. (*d*) A mature spermatid labeled with ABY SP56. The MOs have formed a distinct body lobe with invaginated membranes and moved to the cell periphery. Note that gold labeling is confined to the MOs and the cell surface. (*e*) A spermatid labeled with ABY TR20. Fibrous bodies are no longer evident; the label is spread throughout the cytoplasm. Bar in *a*, 0.1 μm; bar in *c*, 0.2 μm; bars in *b*, *d*, and *e*, 0.5 μm.

tids (34). As a consequence, protein synthesis must be completed before the spermatids bud off the secondary spermatocyte. We have shown that *C. elegans* sperm use a unique structure, the FB–MO complex, to ensure that cell-specific proteins synthesized early in spermatogenesis are delivered to the developing spermatid and, eventually, localized properly in the fully differentiated spermatozoon.

The use of gold-labeled antibodies as probes has shown that both cytoplasmic and membrane proteins are transported in the FB–MO complex. This feature simplifies morphogenesis by allowing proteins destined for separate cellular compartments to be shuttled about in a single, prefabricated unit. However, this strategy demands precise construction of the FB–MO complex, and positioning of specific proteins at selected sites within that complex, through an intricate series of steps.

The membranous organelles, under a variety of names (reviewed in reference 20), are prominent components of sperm of a variety of species of nematodes. Most investigators have agreed that the MOs are formed from the Golgi complex (2, 19, 20, 24, 33, 40). Therefore, the assembly of the antigen recognized by ABY SP56 into the MO probably follows the routine taken by many membrane and secretory proteins in higher eukaryotic cells, starting with co-translational insertion into the endoplasmic reticulum followed by sorting in the Golgi complex (reviewed in references 5, 30, and 31). The antigen in the lumen of the head of the MO exhibits the location and fate expected for a secretory protein. The other population of antigen, in the body of the MO, is assembled into the membrane bilayer and remains there throughout spermatogenesis. Because of their distinctly different locations and fates, these two populations of antigen are probably assembled into the MO via separate pathways.

Spermatocytes also assemble antigen recognized by ABY SP56 into membrane-bound, electron-lucent vesicles. We found vesicles that exhibit the same morphology and labeling pattern at two stages in development; first, in primary spermatocytes and, later, at the junction between the residual body and the budding spermatids. In the latter stage, the vesicles fuse with the plasma membrane to separate the spermatids from the parent cell. It is likely that the vesicles in primary spermatocytes also transport membrane components to the cell surface and, therefore, account for the appearance of CGP–ABY SP56 labeling on the plasma membrane early in development.

If our interpretation is correct then there are three distinct pathways for assembling and localizing antigen recognized by ABY SP56 in spermatocytes. ABY SP56 binds to more than

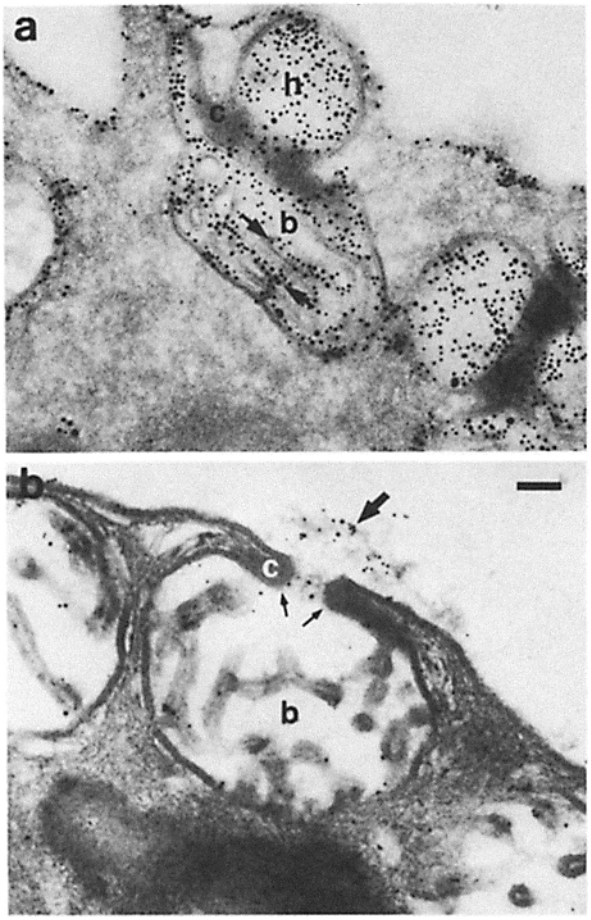

Figure 8. Structure and labeling pattern of MOs before and after fusion. (*a*) An unfused MO consisting of a head (*h*), collar (*c*), and body (*b*) in an ABY SP56-labeled spermatid. Note that the gold particles lie adjacent to the membrane bilayers in the body lobe so that lines of particles parallel profiles of cross-sectioned membrane (arrows). (*b*) A fused MO in a spermatozoon. ABY SP56 labels the fibrous material (large arrow) that surrounds and extends into the fusion pore and also labels the remaining membranes in the body. The head of the MO has disappeared. The collar (*c*) and body (*b*) are still evident although much of the invaginated membrane has been emptied from the body. Note that the plasma membrane and outer body membrane are continuous (small arrows) through the fusion pore. This cell was, in general, less heavily labeled than the one shown in *a*, thus accounting for the difference in gold particle concentration. Bar, 0.1 μm.

eight spots on immunoblots of sperm proteins separated on two-dimensional SDS polyacrylamide gels (38). Thus, different polypeptides that share a common epitope could follow independent routes to different destinations within the cell. Because we do not have antibodies that discriminate among the antigens, we cannot assign individual polypeptides to specific cellular locations and cannot rule out the possibility that all eight polypeptides follow identical routes to the same locations.

Several investigators have noted fibrous bodies associated with the MOs in developing nematode sperm (reviewed in references 20 and 33). Wolf et al. (40) suggested that in *C. elegans* the fibrous bodies form independently as double membrane-bound organelles that later fuse with the MOs.

Table I. Morphometric Comparison of Membrane Surface Areas in Membranous Organelles

Membrane	Surface area (μm^2)*	
	Unfused	Fused
Head	1.3 ± 0.3	—
Outer body	3.3 ± 0.5	3.5 ± 0.6
Invaginations	6.6 ± 0.7	3.7 ± 0.7
Total	11.2 ± 1.2	7.2 ± 1.3

* Based on 484 unfused membranous organelles in both spermatids and spermatozoa and 175 fused membranous organelles in spermatozoa.

Table II. Morphometric Comparison of Membrane Surface Areas in Spermatids and Spermatozoa

Membrane region	Surface area (μm^2)*	
	Spermatid	Spermatozoon
Plasma region	147 ± 12	158 ± 13
Membranous organelles		
Unfused	291 ± 28	109 ± 16
Fused	—	98 ± 10
Total	291 ± 28	207 ± 29

* Based on 66 spermatid profiles and 64 spermatozoan profiles from the same section.

Our observations show that this is incorrect. We found that MO construction starts before fibrous body formation, that the fibrous bodies form within the confines of the body of the MO and, that the membranes surrounding the fibrous body are MO-derived. Therefore, we agree with Ugwanna and Foor (33) that a stable FB–MO complex is established while the two organelles are being assembled.

The sensitivity of immunogold labeling allowed us to detect accumulation of MSP as small amorphous aggregates surrounded by the body of the MO. We could not detect MSP outside the MO and, thus, could not determine where the protein is synthesized or how it accumulates within the MO. The filaments characteristic of mature fibrous bodies did not appear until the growing mass of MSP was enveloped by the membranes of the MO. Therefore, as observed for other fibrous proteins (reviewed in reference 18), a critical concentration of MSP may be necessary to initiate filament polymerization. The fibrous bodies continue to enlarge even after they are wrapped by MO membrane. Sections through fibrous bodies often reveal gaps in the surrounding membranes (see Fig. 5*d*). These gaps must allow newly synthesized MSP to continue to accumulate and polymerize in the growing fibrous body.

We do not know how the FB–MO complexes are segregated to the budding spermatids, although the conventional spindle of microtubules that appears during meiosis (34) is a likely candidate. Whatever the underlying mechanism, the segregation of organelles during construction of the spermatids is striking. The FB–MO complexes, mitochondria, and haploid nuclei segregate to spermatids while all microtubules and microfilaments remain in the residual body (Ward, S., unpublished observations). This segregation of cytoplasmic components is not reflected by at least one cell surface component because ABY SP56-labeled plasma membrane proteins do

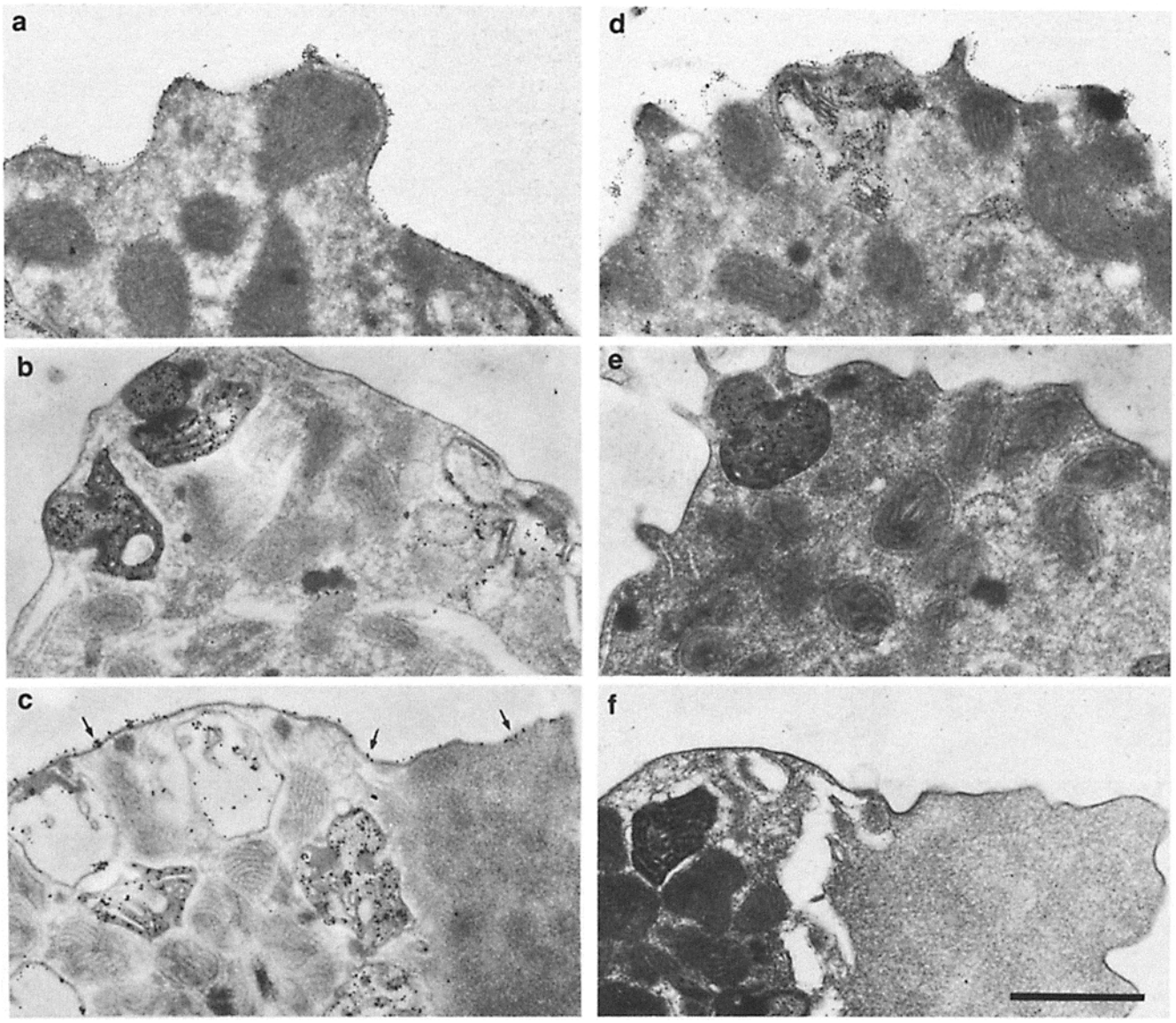

Figure 9. Effect of pronase treatment on labeling of the surface of wild-type (*a–c*) and *fer-1* mutant (*d–f*) sperm with ABY SP56. (*a* and *d*) Control spermatids not treated with pronase. Antibody labels the plasma membrane and intact MOs in the cytoplasm in both wild-type and mutant cells. (*b* and *e*) Pronase-treated spermatids. The antibody labels the MOs but not the plasma membrane in either wild-type or mutant cells. (*c* and *f*) Spermatozoa obtained by monensin activation of a pronase-treated spermatids. In the wild-type cell (*c*), MOs have fused with the plasma membrane, and CGP–ABY SP56 labeling has reappeared on the cell surface (arrows). The MOs have failed to fuse with plasma membrane in the *fer-1* mutant spermatozoon (*f*), and the plasma membrane is unlabeled. Bar, 1 μm.

not rearrange during spermatid formation and are left behind on the residual body. Interestingly, our previous studies (27, 28) have shown that later in development, during the transition from spermatid to spermatozoon, surface proteins undergo substantial rearrangement exhibited first as random migration over the spermatid surface and later, after pseudopod extension, as continuous centripetal movement over the pseudopod surface but not the cell body.

Separation of the spermatid from the residual body triggers a series of four rapidly occurring changes in the FB–MO complex: separation of the two organelles, packing of the membranous parts of the MO into a distinct lobe, movement of the MOs to the cell periphery, and disassembly of the fibers in the fibrous body (34). We do not know what triggers these events or even if a single signal is involved. Presumably these changes must occur before the cell can undergo spermiogenesis because we have found that monensin treatment does not activate pseudopod formation by spermatids still attached to a residual body but nearby fully detached spermatids activate normally.

The separation of the fibrous bodies and the MOs allows the membrane and cytoplasmic components transported in the FB–MO complex during development to segregate to their separate compartments in the mature cell. Separation denudes the fibrous body so that depolymerization of the filaments deposits MSP directly into the cytoplasm. Previous investigators have suggested that the components of the fibrous body are involved in the crawling movement characteristic of nematode sperm (see, for example, reference 33). We have shown that MSP does eventually localize in the spermatozoon

pseudopod and our previous studies (22, 25, 26) established that the pseudopod propels sperm locomotion. However, the role of MSP, if any, in sperm motility remains to be established.

When the FB–MO complex disassembles, the body of the MO reorganizes into a discrete lobe, but the final positioning of the components in the MO does not occur until the organelle fuses with the plasma membrane. The function of MOs in nematode sperm has been debated extensively (see reference 20). Our results establish that one role is to provide new surface proteins for the spermatozoon. After fusion, the plasma membrane and the remaining MO membrane are continuous so the components stored in the MO probably reach the surface by flowing laterally through the bilayer. Before fusion of the MOs with the surface, we never found CGP-ABY SP56 labeling of the membrane surrounding the head of MOs even though the body membranes labeled extensively. Thus, a barrier must prevent intermixing of membrane components between the two parts of the organelle during development but that barrier must break down after fusion to allow the body membrane components access to the plasma membrane.

This study has demonstrated that sperm-specific proteins recognized by two antibodies are transported through development in the FB–MO complex. It is likely that other sperm-specific gene products are packaged in the same structure. The FB–MO complexes occupy nearly the entire non-nuclear, non-mitochondrial volume of the budding spermatid (see Fig. 6, *a* and *d*) and, therefore, must contain most of the non-nuclear, non-mitochondrial proteins. If this is the case, then to a large extent, the final structure of nematode spermatozoa is determined early in development by the way specific components are assembled into the fibrous bodies and the membranous organelles.

We thank Tom Fellers for assistance with electron microscopy and Linda Mathews for preparing the manuscript.

This work was supported by U. S. Public Health Service, National Institutes of Health Grant No. GM-29994-03 to T. M. Roberts and GM-25243 to S. Ward.

Received for publication 16 July 1985, and in revised form 29 October 1985.

References

1. Baigent, C. L., and G. Muller. 1980. A colloidal gold prepared with ultrasonics. *Experientia.* 36:472–473.

2. Beams, H. W., and S. S. Sekhon. 1972. Cytodifferentiation during spermiogenesis in *Rhabditis pellio. J. Ultrastruct. Res.* 38:511–527.

3. Bellve, A. R. 1979. The molecular biology of mammalian spermatogenesis. *In* Oxford Reviews in Reproductive Biology. Volume I. C. A. Finn, editor. Clarendon, Oxford, England. 159–261.

4. Bennett, D. 1975. The T-locus of the mouse. *Cell.* 6:441–454.

5. Blobel, G. 1980. Intracellular protein topogenesis. *Proc. Natl. Acad. Sci. USA.* 77:1496–1500.

6. Brenner, S. 1974. The genetics of *Caenorhabditis elegans. Genetics.* 77:71–94.

7. Brown, D. D. 1981. Gene expression in eukaryotes. *Science (Wash. DC).* 211:667–674.

8. Burghardt, R. C., and W. E. Foor. 1978. Membrane fusion during spermiogenesis in *Ascaris. J. Ultrastruct. Res.* 62:190–202.

9. Carlemalm, E., R. M. Garavito, and W. Villiger. 1982. Resin development for electron microscopy and an analysis of embedding at low temperature. *J. Microsc.* 126:123–143.

10. Distel, R. J., K. C. Kleene, and N. B. Hecht. 1984. Haploid expression of a mouse testis -tubulin gene. *Science (Wash. DC).* 224:68–70.

11. Fawcett, D. W. 1975. The mammalian spermatozoon. *Dev. Biol.* 44:394–436.

12. Gold, B., L. Stern, F. M. Bradley, and N. B. Hecht. 1983. Gene expression during mammalian spermatogenesis II. Stage-specific differences in mRNA populations. *J. Exp. Zool.* 225:123–134.

13. Hodgkin, J., H. R. Horovitz, and S. Brenner. 1979. Non-disjunction mutants of the nematode *Caenorhabditis elegans. Genetics.* 91:67–94.

14. Iatrou, K., and G. H. Dixon. 1978. Protamine messenger RNA: its life history during spermatogenesis in rainbow trout. *Fed. Proc.* 37:2526–2533.

15. Iatrou, K., A. W. Spira, and G. H. Dixon. 1978. Protamine messenger RNA: evidence for early synthesis and accumulation during spermatogenesis in rainbow trout. *Dev. Biol.* 64:82–98.

16. Kirschner, M. W. 1982. Microtubules and their role in cell, tissue and organismal polarity. *In* Developmental Order: Its Origin and Regulation. S. Subtelny and P. B. Green, editors. Alan R. Liss, Inc., New York. 117–132.

17. Kleene, K. C., R. J. Distel, and N. B. Hecht. 1983. cDNA clones encoding cytoplasmic poly(A)$^+$ RNAs which first appear at detectable levels in haploid phases of spermatogenesis in the mouse. *Dev. Biol.* 98:455–464.

18. Korn, E. D. 1978. Biochemistry of actomyosin-dependent cell motility (a review). *Proc. Natl. Acad. Sci. USA.* 75:588–599.

19. Lee, D. L. 1971. The structure and development of the spermatozoon of *Heterakis gallinarum* (Nematoda). *J. Zool.* 164:181–187.

20. McLaren, D. J. 1973. The structure and development of the spermatozoon of *Dipetalonema viteae* (Nematoda: Filariodea). *Parasitol.* 66:447–463.

21. Monesi, V., R. Geremia, A. D'Agostino, and C. Boitani. 1978. Biochemistry of male germ cell differentiation in mammals: RNA synthesis in meiotic and postmeiotic cells. *Curr. Top. Dev. Biol.* 12:11–36.

22. Nelson, G. A., T. M. Roberts, and S. Ward. 1982. *Caenorhabditis elegans* spermatozoan locomotion: amoeboid movement with almost no actin. *J. Cell Biol.* 92:121–131.

23. Nelson, G. A., and S. Ward. 1980. Vesicle fusion, pseudopod extension, and amoeboid motility are induced in nematode spermatids by the ionophore monensin. *Cell.* 19:457–464.

24. Pasternak, J., and M. R. Samoiloff. 1972. Cytoplasmic organelles present during spermiogenesis in the free-living nematode *Panagrellus silusiae. Can. J. Zool.* 50:147–151.

25. Roberts, T. M. 1983. Crawling *Caenorhabditis elegans* spermatozoa contact the substrate only by their pseudopods and contain 2-nm filaments. *Cell Motil.* 3:333–347.

26. Roberts, T. M., and G. Streitmatter. 1984. Membrane-substrate contact under the spermatozoon of *Caenorhabditis elegans*, a crawling cell that lacks filamentous actin. *J. Cell Sci.* 69:117–126.

27. Roberts, T. M., and S. Ward. 1982. Membrane flow during nematode spermiogenesis. *J. Cell Biol.* 92:113–120.

28. Roberts, T. M., and S. Ward. 1982. Centripetal flow of pseudopodial surface components could propel the amoeboid movement of *Caenorhabditis elegans* spermatozoa. *J. Cell Biol.* 92:132–138.

29. Romano, E. L., C. Stolinski, and N. C. Hughes-Jones. 1975. Distribution and mobility of the A, D, and C antigens on human red cell membranes: studies with a gold-labelled antiglobulin reagent. *Brit. J. Hematol.* 30:507–516.

30. Rothman, J. E. 1982. The Golgi apparatus: roles for distinct 'cis' and 'trans' compartments. *Ciba Found. Symp.* 92:120–137.

31. Sabatini, D. D., G. Kreibich, T. Morimoto, and M. Adesnik. 1982. Mechanisms for the incorporation of proteins in membranes and organelles. *J. Cell Biol.* 92:1–22.

32. Solomon, F. 1981. Specification of cell morphology by endogenous determinants. *J. Cell Biol.* 90:547–553.

33. Ugwanna, S. C., and W. E. Foor. 1982. Development and fate of the membranous organelles in spermatozoa of *Ancylostoma caninum. J. Parasitol.* 68:834–844.

34. Ward, S., Y. Argon, and G. A. Nelson. 1981. Sperm morphogenesis in wild-type and fertilization-defective mutants of *Caenorhabditis elegans. J. Cell Biol.* 91:26–44.

35. Ward, S., and M. Klass. 1982. The location of the major protein in *Caenorhabditis elegans* sperm and spermatocytes. *Dev. Biol.* 92:203–208.

36. Ward, S., E. Hogan, and G. A. Nelson. 1983. The initiation of spermiogenesis in the nematode *Caenorhabditis elegans. Dev. Biol.* 98:70–79.

37. Ward, S., T. M. Roberts, G. A. Nelson, and Y. Argon. 1982. The development and motility of *Caenorhabditis elegans* spermatozoa. *J. Nematol.* 14:259–266.

38. Ward, S., T. M. Roberts, S. Strome, F. M. Pavalko, and E. Hogan. 1985. Monoclonal antibodies that recognize a polypeptide antigenic determinant shared by multiple *Caenorhabditis elegans* sperm-specific proteins. *J. Cell Biol.* 102:1778–1786.

39. Weibel, E. R. 1973. Stereological techniques for electron microscopic morphometry. *In* Principles and Techniques of Electron Microscopy. Volume 3. M. A. Hayat, editor. Van Nostrand Reinhold Co., New York. 239–296.

40. Wolf, N., D. Hirsh, and J. R. McIntosh. 1978. Spermatogenesis in males of the free-living nematode *Caenorhabditis elegans. J. Ultrastruct. Res.* 63:155–169.